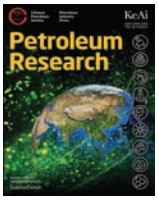
Petroleum Research 11 (2026) 72–83

Contents lists available at ScienceDirect

Petroleum Research

journal homepage: http://www.keaipublishing.com/en/journals/petroleum-research/



Full Length Article

DLVO-based prediction of critical pH for fines migration in sandstone reservoirs



Elmira Dalabayeva [a], Peyman Pourafshary [a, *], Rizwan Muneer [b]

[a] School of Mining and Geosciences, Nazarbayev University, Astana, Kazakhstan
[b] College of Science and Engineering, Hamad Bin Khalifa University, Doha, Qatar

ARTICLE INFO

Article history:
Received 4 March 2025
Received in revised form
4 June 2025
Accepted 4 June 2025
Available online 10 June 2025

Keywords:
Fines migration
DLVO theory
Critical pH
Sandstone reservoirs
Formation damage

ABSTRACT

Fines migration is a formation damage mechanism that occurs in sandstone formations due to the incompatibility between injected fluids and in situ fluids during various operations such as water flooding, drilling, and completion. Fines migration can lead to production problems such as pore blockage and reduced permeability. Parameters such as salinity, pH, and flow rate affect the forces between fines and the rock surface, potentially triggering fines migration. Therefore, predicting the conditions that lead to fines release and migration is critical for ensuring safe operations. Enhanced oil recovery methods, such as low-salinity water injection and alkaline flooding, alter the salinity and pH within the formation, affecting the electrostatic interaction forces between fines and the rock surface. Hydrodynamic forces also influence fines release. Therefore, predicting the initiation of fines migration requires considering and analyzing all these forces. In this work, a modified method based on DLVO theory was developed to predict the critical pH for fines release. The model estimates the onset of fines migration by evaluating electrostatic and hydrodynamic repulsive and attractive forces. For example, the model predicted critical pH values of 8 and 10 at salinities of 0.2 M NaCl and 0.25 M NaCl, respectively. Several core flooding tests were conducted to measure the critical pH for fines release, validating the developed model. The experimental observations showed good agreement with the model, with an error of approximately 13% in predicting the critical pH. The developed approach enables the identification of optimal brine conditions to mitigate fines migration and formation damage, which is a significant finding for enhanced oil recovery and production operations.

© 2025 Chinese Petroleum Society. Publishing services by Elsevier B.V. on behalf of KeAi Communications Co. Ltd. This is an open access article under the CC BY-NC-ND license (http://creativecommons.org/licenses/by-nc-nd/4.0/).

1. Introduction

Formation damage is a significant challenge in managing oil reservoirs, as it impacts recovery and the long-term productivity of fields. It occurs due to unfavorable interactions between invaded fluids, rock particles, and in situ reservoir fluids, often triggered by operations such as drilling, completion, and injection (Chequer et al., 2021; Khilar and Fogler, 1984). Physical or chemical changes within the reservoir caused by formation damage can lead to decreased hydrocarbon recovery and significant management challenges (Al-Sarihi et al., 2018; Karazincir et al., 2017; Russell et al., 2018).

One mechanism of formation damage is the migration of fine particles (Al-Sarihi et al., 2018). According to Muneer et al. (2022), fines migration, which can significantly reduce reservoir permeability and productivity, represents a critical challenge in water flooding and enhanced oil recovery (EOR) operations. Key physical and chemical properties of the injected fluid, such as salinity and pH, directly influence the reservoir's equilibrium state and the behavior of fines (Barnaji et al., 2016; Mehdizad et al., 2022). For example, low-salinity water flooding (LSWF) can destabilize fines by weakening the adhesive forces between clay particles and rock surfaces due to alterations in ionic strength (Agi et al., 2023; Mehdizad et al., 2022; Wang et al., 2021). Similarly, changes in the pH of injected fluids can modify mineral dissolution and precipitation processes by altering the surface charges of mineral particles, leading to fines detachment.

One of the largest sources of oil and gas reserves is sandstone reservoirs, which predominantly consist of sand grains and clay

* Corresponding author.
E-mail address: Peyman.Pourafshary@nu.edu.kz (P. Pourafshary).
Peer review under the responsibility of Editorial Office of Petroleum Research.

https://doi.org/10.1016/j.ptlrs.2025.06.002
2096-2495/© 2025 Chinese Petroleum Society. Publishing services by Elsevier B.V. on behalf of KeAi Communications Co. Ltd. This is an open access article under the CC BY-NC-ND license (http://creativecommons.org/licenses/by-nc-nd/4.0/).

particles on rock surfaces, with oil or water occupying the void pore spaces within the rock matrix (Chavan et al., 2019). However, under certain chemical conditions during oil production, clay particles in sandstone may become unstable and block the fluid channels (Gong et al., 2016). For example, during the alkaline flooding in sandstone reservoirs, injected fluids' pH influences the sand fine system. A rise in pH reduces the negative charge of surface-active components on clay particles, thereby decreasing repulsive forces and increasing the likelihood of detachment. This destabilization is exacerbated by the ionic strength of the injected water. For example, in salt-free solutions, the absence of counter-ions enhances clay destabilization, leading to permeability loss at a lower pH of 2.6, as reported by Vaidya and Fogler (1992), compared to 3.6 as observed by Kia et al. (1984). Hence, fines detachment is related to a combination of salinity and pH conditions.

Muneer et al. (2020) found that high pH conditions promote particle mobilization due to increased repulsive forces. Experiments using salt solutions, such as NaCl, under high-pH conditions confirmed this phenomenon (Muneer et al., 2020; Rosenbrand et al., 2015) They observed that clay particles, such as kaolinite, interact with OH^- ions, and as the surface charge of clay particles becomes less negative, OH^- diffuses away, reducing repulsive forces. Ma et al. (2020) demonstrated that under neutral pH conditions (pH = 7), clay surfaces adsorb both OH^- and cations, leading to a more dispersed cation distribution and increasing repulsive forces between clay particles and the rock surface, contributing to clay swelling.

Another factor influencing permeability reduction during alkaline flooding is the flow rate of the injected fluid. Bradford et al. (2013) and Karazincir et al. (2017) suggested that clay particle mobility increases under high-velocity fluid flow conditions. During high-rate fluid injection, clay particles are released, migrate into the pores, and become trapped, leading to further permeability reduction (Khilar and Fogler, 1984; Musharova et al., 2012). Muneer et al. (2023) suggested that a high pH value may also lead to fines release even at low fluid injection rates. However, Johnson et al. (2009) observed that under buffered saltwater conditions, neutral pH has a negligible effect on fines migration, regardless of velocity.

The critical values of velocity, temperature, pH, ionic strength, and particle repulsion significantly influence fines release in reservoirs. Moreover, the critical value marks the onset of fines release (You et al., 2019). When the properties of the injected fluid exceed their critical values, fines migration begins. This raises the question of how to determine the potential for fines migration. For instance, Muneer et al. (2020, 2022) identified critical factors through modeling, which were later validated by experimental studies.

To examine the effect of water salinity on particle release and migration, researchers used the concept of Critical Salinity Concentration (CSC). When water salinity falls below the CSC, fines are released and subsequently mobilized from the rock surface (Khilar and Fogler, 1984; Kia et al., 1987; Mansour et al., 2020). This hypothesis was experimentally validated by Muneer et al. (2020), who conducted chemical analyses of rock and fluid compositions. The CSC was predicted using the Derjaguin–Landau–Verwey–Overbeek (DLVO) model, which calculates the energy required for particle detachment and movement within a rock system.

Musharova et al. (2012) and Yan et al. (2015) applied DLVO theory in their experiments to evaluate the forces influencing particle behavior. Their findings suggest that DLVO theory is suitable for describing interactions in fine-sand-brine systems. According to their study, repulsive forces significantly contributed to reduced fines migration and lower permeability. The verified model of DLVO is then used to predict fines detachment during coreflood tests, which have demonstrated that under certain conditions (e.g., changes of temperature, salinity, or pH), repulsion force is dominant, especially in matrix clays systems.

The DLVO theory provides a framework for understanding the impact of these forces, enabling the estimation of formation damage and its control strategies. While previous scientific research has thoroughly studied the effects of salt concentrations and ionic strength using DLVO theory, the main idea of this work is to predict fines migration initiation at different pH levels and under varying conditions of flow rate.

Critical pH modeling is important since it helps to avoid the formation of damage at alkaline flooding into the sandstone reservoirs by controlling the surface charge interaction between the rock surface and fines. The electrostatic repulsion reaches its maximum state at the critical pH level, so the net surface potential reaches zero or becomes positive, which leads to detaching the fines. Therefore, the objective of this thesis is to predict critical pH and flow rate during the water injection for sandstone reservoirs, using DLVO modeling. To validate the model, a comparison with actual experimental data was made.

2. Theory

DLVO theory provides a conceptual framework for describing interactions between surfaces separated by a liquid, particularly in colloidal systems. This theory is based on the laws of intermolecular forces of electromagnetic origin (Hernandez, 2023). According to DLVO theory, interactions are governed by two opposing forces: attraction and repulsion. Khilar and Fogler (1984), Trefalt and Borkovec (2014), and Muneer et al. (2020) noted that the cumulative effects of attractive van der Waals forces (V_{LVW}), repulsive electric double-layer forces (V_{EDL}), and Born forces influence particle movement and can control fines migration. To quantify this phenomenon, Sourani et al. (2014) evaluated the forces between spherical and planar surfaces, representing fine particles and sand grains, respectively, providing a framework for understanding particle behavior in such systems.

Attractive forces between particles exist when they are close. The distance at which molecules, atoms, and particles attract each other does not depend on covalent or ionic interactions but rather on attraction energy (Khilar and Fogler, 1984). This energy decreases rapidly and has an action range of less than 10 nm. The fluctuating dipoles of atoms generate electrostatic forces, and the negative sign of van der Waals potential energy indicates attractive interactions (Gregory, 1981). According to Ohshima and Takeda (2024), the Hamaker constant parameter is used to measure the strength of van der Waals forces between materials and represents the interaction surfaces.

Repulsive electrostatic forces result from the distribution of charge on surfaces and in the surrounding liquid, particularly when the surfaces are electrically charged. Moving ions in a solution with a specific salinity creates ionic layers around charged sand grains and the tiny, similarly charged particles dispersed throughout the solution. From the surrounding brine, positively or negatively charged particles are attracted to oppositely charged ions, forming a compact yet dynamic layer (Loeb et al., 1961; Muneer et al., 2022). The excess charge is balanced by an equivalent number of oppositely charged ions from the brine solution, establishing a secondary layer known as the diffuse layer. The ions in this diffuse layer move independently between the brine and the diffuse layer itself (Elimelech, 1995).

To differentiate between the compact and diffuse layers, zeta potential is used in DLVO modeling. Generally, the formulation considers two boundary conditions: either one surface maintains a constant charge density while the other maintains a constant potential, or both sand grains and fine particles possess a fixed charge or surface potential (Ali et al., 2022). Compared to surface charge measurements, zeta potential is a more practical parameter for identifying fines migration (Muneer et al., 2020).

Another repulsive force influencing clay particle migration is the Born repulsive potential. According to Muneer et al. (2022), Born repulsion occurs when particles are extremely close together, causing their electron clouds to overlap. However, if the distance between particles exceeds 1 nm, the effect becomes negligible (Mansour et al., 2020; Muneer et al., 2022; Yang et al., 2022). Additionally, Israelachvili (2011) supports van der Waals theory, which states that when the separation between surfaces exceeds 5 nm, the Hamaker constant remains effective. However, if the separation distance falls below 3 nm, the effect decreases by approximately 25%, aligning with theoretical expectations. In such cases, Born repulsion can be considered negligible. Yang et al. (2022) distinguished Born repulsion from EDL by its lower sensitivity to salinity. This distinction can be explained using DLVO parameters: while EDL is represented by zeta potential, which is directly influenced by salinity, Born repulsion is determined by the Hamaker constant, which depends on particle size (Barouch et al., 1987; Schumacher and van de Ven, 1987).

Hydrodynamic forces also play a crucial role in the release of fines from rock surfaces. Factors such as particle size, injection fluid velocity, salinity, and pH significantly influence this process. Muneer et al. (2023) investigated fines migration under both low and high injection rates, taking into account brine salinity and particle size. At low injection rates, electrostatic forces were found to dominate the detachment of clay particles from sand, and the forces exerted by fluid movement on fine particles are negligible.

Fig. 1 shows how fine particles detach and move through porous media based on forces that have an impact on formation damage. The relationship between the hydrodynamic (lift F_l, and drag F_d) forces, gravity force (F_g), and electrostatic force (F_e) regulates particle mobility. The DLVO theory demonstrates that this value results from the combined powers of electrostatic repulsion alongside van der Waals attraction. However, when the hydrodynamic forces become higher than the gravitational and electrostatic forces, there is a possibility that fines start to release even when pH or salinity are within the critical thresholds. During high flow-rate injection, the increased shear stress exerted by fluid flow on the rock surface becomes the dominant factor driving particle migration. As a result, hydrodynamic forces significantly increase, overpowering electrochemical forces and leading to particle detachment.

The total interaction energy considering both electrostatic and hydrodynamic forces can be written as:

$$V = V_{LVW} + V_{EDL} + V_{BR} + V_{hydro} \tag{1}$$

$$V_{LVW} = -A\frac{a_p}{12H} \tag{2}$$

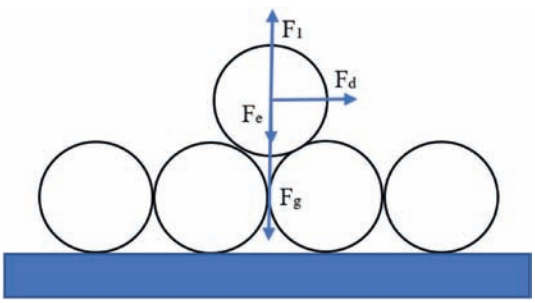


Fig. 1. Acting forces on a fine particle on the sand surface (Sourani et al., 2014).

$$V_{EDL} = 2\pi\varepsilon_m\varepsilon_0 a_p z^2 \ln\left(1+e^{\frac{-h}{k^{-1}}}\right) \tag{3}$$

$$V_{BR} = \frac{A_H}{7560}\left(\frac{\sigma}{a_p}\right)\left[\frac{8+H}{(2+H)^7}+\frac{6-H}{H^7}\right] \tag{4}$$

where V_{LVW}, V_{EDL}, and V_{BR} are van der Waals, electric double layer, Born forces, and hydrodynamic forces, respectively. However, van der Waals attraction may vary based on different particles and the geometry. Gregory (1981) suggested Equation (2) to calculate the van der Waals force for kaolinite platelets.

Fine detachment during the high flow rate can be affected by several forces, such as hydrodynamic or drag force (F_d), lift force (F_l), electrostatic force (F_e), and gravity force (F_g), these forces are calculated using Equations (5)–(7), respectively (Saffman, 1965; O'Neill, 1968; Chrysikopoulos and Syngouna, 2014). The electrostatic force is found by using the separation distance and taking the derivative of the total energy values. Hydrodynamic forces have a significant role during the injection with a high rate because of flow rate fines, detachment may occur earlier than at critical pH.

$$F_d = 1.7009 \times 6\pi\mu r_f v_s \tag{5}$$

$$F_l = 81.2\sqrt{\rho\mu}\left(r_f v_s\right)^{1.5} \tag{6}$$

$$F_g = \frac{4}{3}\pi r_f^3\left(\rho_f-\rho\right)g \tag{7}$$

Equation (8) is used to analyze the velocity profile of fluid flow in porous media around fine particles. Specifically, it aligns with the velocity distribution in the creeping flow regime, such as that governed by Stokes flow, where inertial forces are negligible compared to viscous forces.

$$v_s = 2v\left(1-\frac{\left(r_p-r_f\right)^2}{r_p^2}\right) \tag{8}$$

Equation (9) defines the conditions for fines release, which occurs when the injection velocity exceeds the critical rate. In this equation, the injection velocity accounts for the relationship between drag forces, lift forces, the external moment of viscous stress, and the fine particle radius.

$$10.21\pi\mu r_f v_s + 81.2\sqrt{\rho\mu}\left(r_f v_s\right)^{1.5} + 7.55\pi\mu v_s > F_g + F_e \tag{9}$$

Equations (8) and (9) were used to make the final equation to generate the critical velocity profile for brine injections in porous media. However, during the low injection rate, the lift forces can be neglected compared to drag forces. Therefore, by considering forces that have an impact on fines detachment, Equation (10) was developed to calculate the critical rate using DLVO modeling (Muneer et al., 2024).

$$v = \left(F_g+F_e\right)\left[\frac{2r_f\left(2r_p-r_f\right)\left(17.75\pi\mu r_f\right)}{r_p^2}\right]^{-1} \tag{10}$$

The DLVO model can be influenced by pH, as it affects the EDL by altering the surface charge of particles. This change can disrupt the balance between attractive and repulsive forces, impacting particle behavior. For example, Muneer et al. (2020) highlighted that high pH levels promote particle repulsion and mobilization. This occurs

due to an increase in negative surface charge and a decrease in zeta potential, which serves as an indicator of surface charge. A decrease in zeta potential confirms the change in surface charge at high pH levels, leading to an increase in electrostatic repulsive forces and the release of fine particles.

It is important to note that the impact of pH may vary across different parts of a material due to differences in charge distribution. Yang et al. (2022) illustrated this variation using kaolinite surfaces as an example. The edge surface of kaolinite interacts with charged hydrogen species (OH^- and H^+), while the face surface maintains a constant negative surface potential. Assef et al. (2014) attributed this effect to colloidal forces between clay particles and sand grains. According to the authors, these forces are influenced by ionic strength and pH, with the edge surface of kaolinite being more pH-sensitive than the face surface. This behavior aligns with DLVO modeling, which links particle interactions to the energy components of these forces.

3. Methodology

DLVO modeling provides a fundamental framework for understanding the colloidal system and its stability, helping to predict the critical pH by modeling the interaction forces between system particles. These forces were analyzed to determine the critical pH values, with fine migration occurring at the point where the net interaction between these forces becomes positive. This work includes both modeling and experimental studies, where core flooding experiments with NaCl brine at varying pH levels were conducted to model surface force interactions and predict the critical pH value of the injection fluid.

3.1. Measurement of parameters to model fines migration by DLVO

The DLVO theory explains fluid-rock interactions and their behavior during various water injection processes at different pH levels. To determine the attractive and repulsive forces within the brine-sand-fines system, the average size of the fines was measured using scanning electron microscopy (SEM), and the zeta potentials of the sand particles were measured using a Zetasizer and subsequently modeled. Additionally, the salinity and pH of each brine sample were carefully considered. van der Waals and electric double-layer forces were calculated using Equations (2) and (3), respectively (Gregory, 1981; Muneer et al., 2020; Sourani et al., 2014). Another repulsive force that may influence fines migration, the Born repulsive potential, was calculated using Equation (4). When the flow rate was high, the model incorporated hydrodynamic forces using Equations (5)–(10). After calculating each repulsive and attractive force, they were quantified using Equation (1) (Mansour et al., 2020; Muneer et al., 2020; Khilar and Fogler, 1984; Trefalt and Borkovec, 2014), and the DLVO model was developed.

The DLVO model was used to predict the migration of fine particles. As an example, cases with salinities of 0.1 M NaCl, 0.2 M NaCl, 0.25 M NaCl, and 0.3 M NaCl were analyzed to determine the critical pH value under low flow rate conditions. For high flow rate conditions, the critical flow rate was determined based on the work of Muneer et al. (2023). Specifically, a salinity of 0.25 M NaCl and pH 7 was used, along with a case where pH was increased to 8 while maintaining the same salinity. Several constant parameters used in the study are shown in Table 1. Brine viscosity and density were measured using an Anton Paar viscometer, while pore and particle radius were measured using scanning electron microscopy. The Hamaker constant was integrated by Muneer et al. (2022) for the kaolinite-sand-brine system. For systems containing other clay minerals, the Hamaker constant should be adjusted to reflect the specific van der Waals interaction properties of the respective clay.

Table 1
Constant parameters that are used for the DLVO application in our study.

Parameter	Symbol	Value
Fluid Temperature	T	297.15 K
Hamaker constant	A_H	3×10^{-21} J
Boltzmann constant	K_B	1.38×10^{-23} JK^{-1}
The dielectric constant of water	ε_m	80
Permittivity of vacuum	ε_o	8.85×10^{-12} $C^2J^{-1}m^{-1}$
Electron charge	e	1.6×10^{-19} C
Avogadro's Number	N_A	6.02×10^{23} mol^{-1}
Atomic collision diameter	σ	5×10^{-10} m
Effective electrostatic force	F_e	3.07×10^{-11} kg m/sec^2
Brine viscosity	μ	0.001121 kg/m sec
Pore radius	r_p	5×10^{-5} m
Kaolinite density	ρ_f	2650 kg/m^3
Brine density	ρ	970 kg/m^3

3.2. Brine preparation

The brine salinity was selected to be higher than the CSC based on previous analysis, following the approach outlined in Muneer et al. (2020, 2022). This selection ensures that the system remains within the regime where wettability alteration and fines mobilization are sensitive to pH changes, allowing for an accurate determination of the critical pH threshold. Therefore, injection brine salinities of 0.2 M NaCl and 0.25 M NaCl were chosen. This restricted salinity range enables to study of small modifications in DLVO forces while remaining able to identify specific detachment thresholds. Brines with different pH values, ranging from 6.5 to 11, were prepared at each salinity level (0.2 M and 0.25 M NaCl) to measure the critical pH. The testing scope included this pH range because it covered both neutral and strongly alkaline conditions that commonly occur with alkaline EOR and low-salinity water flooding operations. Laboratory analysis of this pH range determines when electrostatic repulsion reaches its minimum point, which results in fines separation from mineral material.

Moreover, these conducted pH values reduce the possible effects of mineral dissolution, which affects the migration rate of fine particles, since an acidic environment contributes to such phenomena more effectively. The dissolution of minerals remained minimal enough to be ignored in the analysis due to experimental conditions. Reagent-grade NaCl (Sigma Aldrich) was dissolved in distilled water using a magnetic stirrer to prepare the brines. The samples were carefully stirred at room temperature, and pH measurements were taken once the readings stabilized. The adjusted pH levels of the NaCl brines are listed in Table 2. For the experimental phase, Berea sandstone core samples were saturated with formation water with a salinity of 76,960 ppm. The composition of the NaCl brine and formation water was adjusted by adding NaOH, and samples with pH values ranging from 6.5 to 11 were prepared at each salinity level.

3.3. Rock preparation

The Upper Berea Sandstone outcrop samples were used to evaluate the modeled critical pH for sandstone reservoirs. Cores

Table 2
Composition of injection brine and formation water.

Ions	Formation water (ppm)	Injection brine (ppm)
Na+	23427	4595
Ca+	4450	0
Mg+	1302	0
Cl-	47781	7092
Total	76960	11687

were selected and characterized to establish grain size, particle size distribution, and chemical composition. The average length and diameter of the samples were 7.5 cm and 3.8 cm, respectively. Mineralogical analysis via XRD revealed that the samples are primarily composed of quartz, with smaller amounts of magnesium oxide (MgO), iron oxide (Fe_2O_3), aluminum silicate (Al_2SiO_5), and aluminum oxide (Al_2O_3), as shown in Table 3. To better understand the rock's composition and its physical and mechanical properties, SEM was employed. The analysis confirmed that silicon has the highest concentration in the Berea outcrop sample.

First, Berea sandstone samples were cut, dried in an oven, and their dry weights were recorded. After saturation, the wet weights were measured to determine porosity, which ranged from 0.192 to 0.194, and liquid permeability, estimated to be between 350 and 400 mD. The core samples were then used for core flooding experiments to validate the model.

3.4. Zeta potential determination

Zeta potential measurements are a valuable method for studying the behavior of colloidal particles in liquids. In this study, Berea sandstone core samples were crushed using a core-crushing apparatus, and the resulting fine powder was sieved through a 40 μm sieve to measure the sand-brine zeta potential. To ensure the sample was representative and free of contaminants, the sand powder underwent multiple cleaning steps using n-hexane, acetone, and distilled water. The samples were then dried in an oven at 60 °C for one day, rinsed with 0.5 M hydrochloric acid, and further cleaned with solutions of 0.2 M and 0.25 M sodium chloride, adjusted with sodium hydroxide, until the adjustment of the required pH.

After 24 h of equilibrium exposure, zeta potentials were measured using Malvern Zetasizer equipment to ensure the correct brine-to-sand particle ratio. The measured zeta potentials for the sand-brine systems were incorporated into DLVO modeling, and pH values were assessed for all samples. While using a Zetasizer to measure zeta potential is a commonly applied experimental method, it has certain limitations. It can be time-consuming, resource-intensive, and difficult to scale for subsurface conditions with a wide range of variables. Therefore, alternative approaches that are both efficient and reliable are needed.

To gain a more comprehensive understanding of zeta potential, an alternative predictive model was developed using the XGBoost (eXtreme Gradient Boosting) machine learning technique, which combines boosting techniques with decision trees. The zeta potential prediction using XGBoost involved several steps: data collection, preprocessing, model training, and evaluation. XGBoost was selected due to its strong predictive performance in most literature and its suitability for small to medium-sized datasets. This made it a practical choice for the current dataset, which includes variables such as pH, ionic strength, ion type, temperature, and medium that exhibit complex non-linear interactions. The use of deep learning models was excluded because such models need extensive datasets to minimize overfitting issues. Moreover, the regularization features built into XGBoost contribute to improved model stability and generalization.

Table 3
Mineralogy of sandstone sample determined by XRD.

Chemical composition	Formula	Weight (%)
Quartz	SiO_2	87.14
Kaolinite	$Al_2Si_2O_5(OH)_4$	6.41
Aluminum oxide	Al_2O_3	3.97
Magnesium oxide	MgO	0.81
Iron oxide	Fe_2O_3	1.67

A dataset of 173 data points was created from our experiments and academic papers where zeta potential had been determined experimentally or through modeling. The temperature range spanned from 15 to 145 °C, with ionic strength varying from 0 to 29,220 ppm for NaCl and 0 to 20,000 ppm for KCl. The dataset also included various porous media, such as Berea sandstone, gray sandstone, Buff sand, clay sand, Bandera, Parker, glass beads, kaolinite, and coal fines. Brine pH values ranged from 1 to 12.

Data preparation for machine learning included normalizing continuous features, such as pH, salinity, temperature, and ionic strength, to a range between zero and one. This normalization step ensured that larger-scale features, like salinity, did not overshadow smaller-scale features, such as pH. Categorical variables, like the type of porous medium, were converted to binary values for compatibility with the model and to ensure interpretability. The finalized dataset was split into three subsets: 70% for training, 15% for validation, and 15% for model performance evaluation. Stratified sampling was applied to ensure a uniform distribution of features across all subsets.

3.5. Core flooding for low-rate fluid flow

A series of coreflood tests using NaCl brine was conducted to measure the critical pH. Each test was performed at room temperature (24 °C), with a back pressure of 260 psi and a confining pressure of 1000 psi. As the system's salinity was reduced from 77,000 ppm to 11,688 ppm (0.2 M NaCl) and 14,610 ppm (0.25 M NaCl), a soaking period between injections was necessary to establish surface force equilibrium. For each test, 2 pore volumes (PV) of the specified NaCl brine were injected at a rate of 0.2 cc/min, followed by a 24-h soaking period. After soaking, brine with the same salinity but an increased pH was injected. The same procedure was repeated using 0.25 M NaCl brine. The low injection rate of 0.2 cc/min was chosen to minimize the effect of hydrodynamic forces on fines migration. The pH was systematically increased from 6.5 to 11 in increments of one.

A schematic image of the coreflood setup is shown in Fig. 2, and the same methodology was applied using 0.25 M NaCl brine. The device analyzes important parameters, which include brine sensitivity, together with critical flow velocity and EOR methods. The device offers controlled operation through computer software that enables both manual and automated management of pumps and valves and data recording. The automated test routines execute through an integrated test sequencer. The isothermal convective air bath contains core components with a core holder and air-operated valves, and an optional fluid separator and plumbing.



Fig. 2. Core flooding system setup for enhanced oil recovery experiments. *Reproduced from* Vinci Technologies.

3.6. Coreflooding experiment at high flow rate

To measure the critical velocity and consider the hydrodynamic forces, the injection rate of brine with salinity above CSC was gradually increased from 0.2 cc/min to 5 cc/min. The test began with an injection of 3 PV of brine at a rate of 0.2 cc/min, after which a soaking period was given to ensure sufficient contact between sand, fine, and injection brine. Then, the same 0.25 M NaCl brine was injected, and the injection rate gradually increased with each 3 PV injection. 3 PV was chosen to see any pressure change in the system. Due to the potential for fine migration, pressure drop values were recorded at each step. The test was carried out to determine the experimental value of the critical flow rate at a higher CSC salinity and lower critical pH.

3.7. Effluent analysis

At the end of each flooding, pressure difference data and effluents were collected at various pH levels of the injected fluid. UV-VIS spectroscopy was employed to analyze the effluent, a method that determines the concentration of compounds in a sample by measuring ultraviolet absorption. By examining the data, the critical pH level and the presence of fine particles can be compared with the results of the DLVO theory, which is supported by higher absorption at specific wavelengths.

4. Results

4.1. Modeling of fines migration by DLVO at a low flow rate condition

4.1.1. Zeta potential measuring and modeling

Zeta potentials for 0.2 M NaCl and 0.25 M NaCl were determined after cleaning the sand particles and dispersing them in brine using a magnetic stirrer and ultrasonic homogenizer. The measured zeta values are shown in Tables 4 and 5, respectively. For other types of brine, the values were modeled by the developed machine learning approach. Model performance evaluation used R^2 coupled with RMSE, along with MAE as metrics. Training performance of the model achieved an R^2 value of 0.93, but testing and validation yielded an R^2 value of 0.91, thus producing an overall R^2 value of 0.92. The model produced its best RMSE of 0.25 on the training data yet showed increased values of 0.3 and 0.28 for validation and testing, respectively, which indicates higher prediction error for new data points. The performance pattern for MAE shows that training results produced 0.19 while validation/testing rates fell between 0.21 and 0.22, and the outcome reached 0.218.

To validate the accuracy of the model's output parameters, experimental values for 0.2 M NaCl and 0.25 M NaCl were compared with the model predictions. The experimental and modeled zeta values are presented in Table 4. The average error between the experimental and the modeled error is 5.97%. The data indicate that zeta potential decreases as the pH of the brine increases, which can be attributed to the presence of additional hydroxide ions in the solution. Furthermore, since zeta potential is influenced by temperature at different pH levels, the measurements were conducted at room temperature to minimize any additional effects on the output values.

Table 4
Comparison of experimental and modeled zeta potential values for 0.2 M NaCl.

Ionic strength	pH	Z (experiment)	Z (model)
0.2 M NaCl	6	−18.2	−17.06
	7	−20.4	−20.69
	8	−23.7	−21.01
	9	−25.8	−22.6
	10	−27.5	−26.04
	11	−28.9	−29.81
	12	−31	−30.41

Table 5
Modeled zeta potential values for 0.25 M NaCl at different pH levels.

Ionic strength	pH	Z (experiment)	Z (model)
0.25 M NaCl	6.5		−16.5
	7.5		−16.97
	8.5	−17.42	−17.38
	9	−18.97	−18.31
	9.5		−23.6
	10	−27.13	−26.86
	10.5		−27.11
	11	−28.43	−28.81

For the brines with a salinity of 0.25 M NaCl, the properties of the samples and the modeled zeta values are shown in Table 5. Similarly, the zeta potential decreases with an increase in pH. To validate the effectiveness of the zeta potential prediction model for different ionic strengths, additional values were modeled, as shown in Fig. 3. A decrease in brine salinity leads to a reduction in zeta potential, similar to the effect of increasing pH toward basic conditions. These changes can result in the expansion of electric double layers and an increase in repulsive forces, which contribute to the migration of fine particles.

4.1.2. DLVO modeling to predict critical pH for the initiation of fines migration

For DLVO modeling, surface forces between fines and sand grains were estimated based on observed zeta potentials under various pH conditions and brine ionic strengths. The total interaction energy of each system was determined using DLVO modeling, as illustrated in Fig. 3. The total interaction energy represents the sum of the attractive and repulsive potentials in the system. The results for the modeled critical pH are shown in Table 7. The critical pH point was identified as the threshold where the attractive forces between fine particles in a sandstone sample and the injected brine are no longer sufficient to counteract the repulsive forces. This imbalance causes particle separation and subsequent migration.

For 0.25 M NaCl injection brine, sand grains, and fines were surrounded by compacted EDL at pH values between 6.5 and 9.5. Under these conditions, the attractive forces outweighed the repulsive forces, resulting in negative total interaction energy,

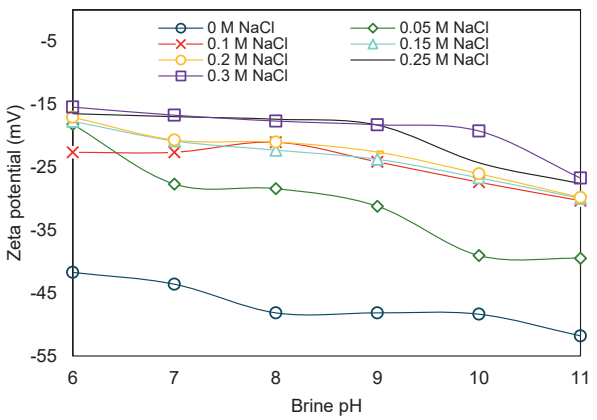


Fig. 3. Zeta potential at different pH and salinity of brines.

which indicates that fines migration does not occur. However, as the pH increased beyond 10, the total interaction energy became positive, reflecting stronger repulsive forces. This shift can be attributed to the increased pH, which enhances the EDL forces between sand and fines. EDL expansion preserves particle separation, thereby increasing repulsive forces. Salinity also influences EDL expansion. At 0.25 M NaCl, the ionic strength prevents significant EDL expansion at low pH due to the higher ion concentration in the brine. Consequently, the critical pH for fines migration was observed to be 10, as the increased hydroxide ion (OH^-) concentration at higher pH levels outweighs the effects of ionic strength.

Testing with 0.2 M NaCl, identified as the CSC for fines migration initiation (Muneer et al., 2022), showed a critical pH of 8. Using the modeled zeta potential values, brine with 0.1 M NaCl salinity exhibited positive total interaction energy starting at pH 7, while brine with 0.3 M NaCl salinity demonstrated negative total interaction energy. At low salinities, EDL expansion is significant because of the reduced ionic strength, leading to greater particle separation. In contrast, at high salinities, increased ion concentration reduces the influence of pH on the system. Thus, at salinities of 0.2 M NaCl and higher, EDL expansion is less pronounced, even at high pH.

Furthermore, DLVO modeling revealed that the Debye length, which varies with ionic strength, contributes to the expansion of repulsive forces. As the EDL strengthens, the Debye length increases, further influencing the system's electrostatic interactions. Debye length values for both brines are shown in Table 6. Moreover, Table 6 shows the maximum values of total interaction energy for each pH of 0.2 and 0.25 M NaCl injected brines to see its dependence on pH. The value is applicable during active surface interactions while migration takes place or is expected to take place. The "Total Interaction Energy barrier" entry blanks are empty for pH values 6.5 and 7.5 for 0.2 M NaCl brine, and from 6.5 to 9.5 values for 0.25 M NaCl brines. It is because there is no interaction barrier to calculate, since particles remain stationary, and the interaction energy model is not triggered. Consequently, it indicates that there is no fine migration for the system.

You et al. (2019) documented how exceeding critical physicochemical thresholds caused clay particle repulsion, which these experiments confirmed during testing of alkaline conditions with elevated salinity levels. Analysis by Hernandez (2023) demonstrates the opposing effects of EDL electrostatic repulsion and van der Waals attraction, which validate the interpreted particle response at the critical pH threshold.

Table 7
Modeled critical pH values at different salinities.

Brine salinity	0.1	0.2	0.25	0.3
Critical pH	7	8	9	11

4.1.3. Validation of fines migration initiation at low flow rates

To evaluate the effect of salinity on coreflood tests involving pH variation, two experiments were conducted at a low flow rate using Upper Berea sandstone samples saturated with formation water at 77,000 ppm. A coreflooding system was employed to monitor pressure changes within the core during brine injection, as these changes play a crucial role in fines dislocation and migration. The tests were performed at a low flow rate to minimize the influence of hydrodynamic forces, ensuring that fines migration was primarily driven by high pH levels rather than flow-induced shear forces. During each test, 2 PV of eight different brines with varying pH levels were injected into the core samples at a flow rate of 0.2 cc/min. Following the initial injection, a 24-h soaking period was applied to allow repulsive and attractive forces to stabilize. This step was necessary due to the reduction in system salinity by 6.5 wt %. Once equilibrium was reached, brine with the same salinity (0.2 M NaCl) was injected sequentially in 2 PV increments to observe the onset of fines release.

As shown in Figs. 4 and 5, no significant change in pressure drop was observed during the injection of brines with pH levels of 6.5 and 7.5. A slight pressure drop occurred at pH 8.5, while a substantial increase in pressure drop was recorded at pH 9 and above. This suggests that at pH levels below 9, attractive forces dominate over repulsive forces, preventing fines migration. The second coreflood test followed the same procedure but used a brine salinity of 0.25 M NaCl. In this case, pressure changes were observed at pH 10, indicating that higher salinity raises the critical pH threshold for fines release. The increased pressure drop during the injection of brine at pH 10 suggests that fines were mobilized from the sandstone surface due to the interaction between brine chemistry and rock properties.

These experiments demonstrate that the critical pH value for fines migration is influenced by salinity, with higher salinity requiring a higher pH to initiate fines release. In both tests, as pH increased, clay particles destabilized and migrated, potentially clogging pore spaces and causing formation damage. After core flooding, effluent samples were analyzed using UV-VIS

Table 6
The values of Debye length and maximum total energy for injected brines.

pH	Salinity (M)	Debye length (nm)	Total interaction energy	The total interaction energy barrier
6.5	0.2	0.685	−14	–
7.5			−13.9	–
8.5			0.13	0.13
9			0.13	0.13
9.5			0.61	0.61
10			2.63	2.63
10.5			4.14	4.14
11			4.34	4.34
6.5	0.25	0.613	−14	–
7.5			−14	–
8.5			−13.9	–
9			−13.9	–
9.5			−13.9	–
10			3.96	3.96
10.5			18	18
11			19.1	19.1

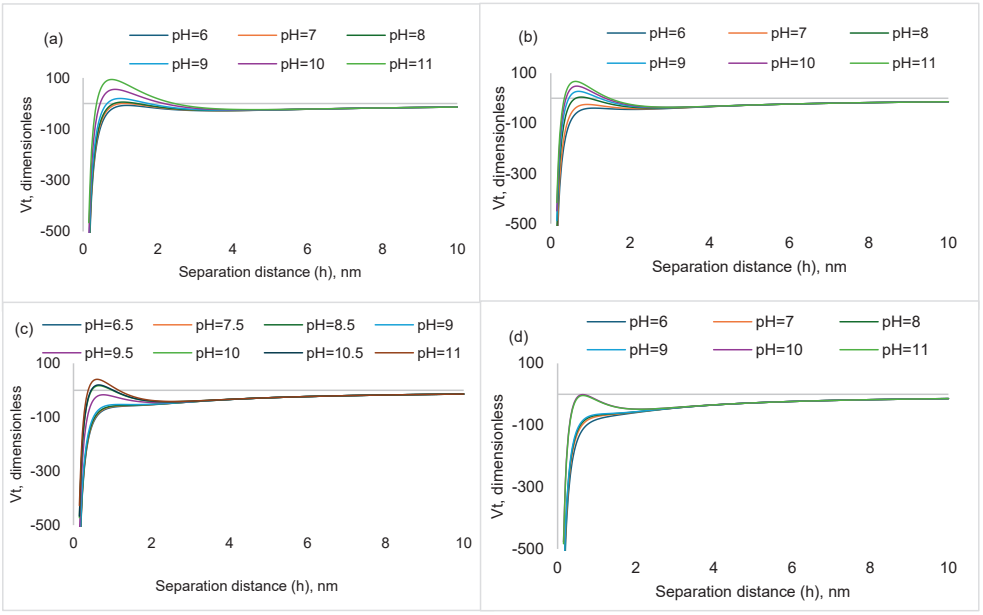


Fig. 4. Prediction of critical pH using DLVO modeling for (a) 0.1 M NaCl (b) 0.2 M NaCl (c) 0.25 M NaCl and (d) 0.3 M NaCl.

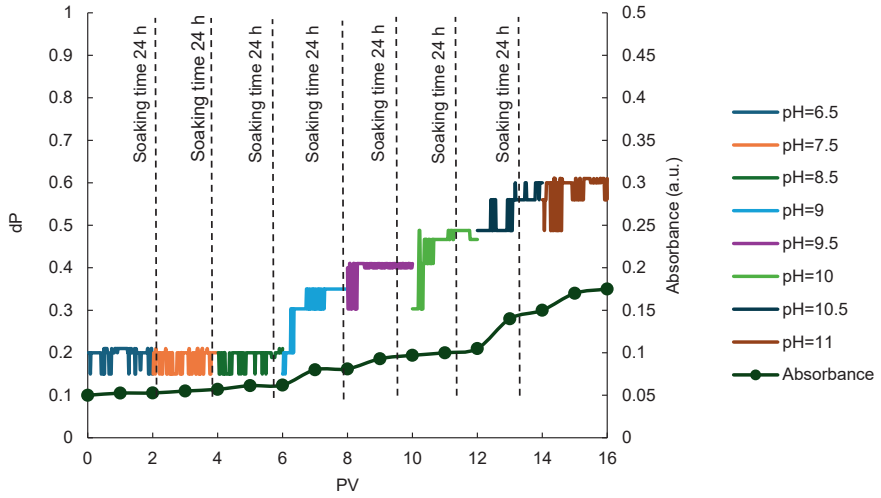


Fig. 5. Pressure drop and light absorbance changes at different pH levels at 0.2 M NaCl salinity.

spectroscopy to detect the presence of fines. This detection relied on measuring the increase in particle concentration in the effluent, which confirmed the pressure drop results and helped identify the critical pH. Spectroscopy results showed a breakthrough in light absorbance between pH 8 and 9 for 0.2 M NaCl, with the highest absorbance value of 0.18 recorded at pH 11 (Fig. 5). For brines with 0.25 M NaCl salinity (Fig. 6), light absorbance increased sharply at pH 10, reaching a peak of 0.15 at pH 11. Since migrating fines are suspended in the produced fluid, they contribute to increased light absorbance in the effluent. The rapid rise in absorbance values may also indicate mineral dissolution, which can impact rock permeability and porosity.

This integrated approach, combining coreflood tests and absorbance measurements, provides a more comprehensive understanding of the interaction between sand, fines, and brine. Overall, the core flooding tests provided experimental confirmation of critical pH values, with high-pressure drops measured at pH 9 for 0.2 M NaCl and pH 10 for 0.25 M NaCl (Table 8). It can be concluded that our developed model can accurately predict the critical pH.

The error estimation in this study provides a confidence level of 95%, indicating that the predicted critical pH value is accurate within this margin. The precision of the measured inputs is sufficient to achieve this level of accuracy, assuming spherical particle shapes and constant ionic strength. Fig. 7 illustrates that the critical pH of the injected brine increases with rising salt concentration. This occurs because alkaline fluids and brines with critical or higher salinity concentrations neutralize the negative charge of the rock, thereby reducing electrostatic repulsion.

EDL is a charged layer surrounding particles in a system, creating an ionic cloud. Its thickness depends on several factors, including surface charge, solution pH, and ionic strength. High-salinity brines contain a greater concentration of ions, which can compress the EDL by neutralizing particle surface charges and reducing repulsion forces. Additionally, elevated salt

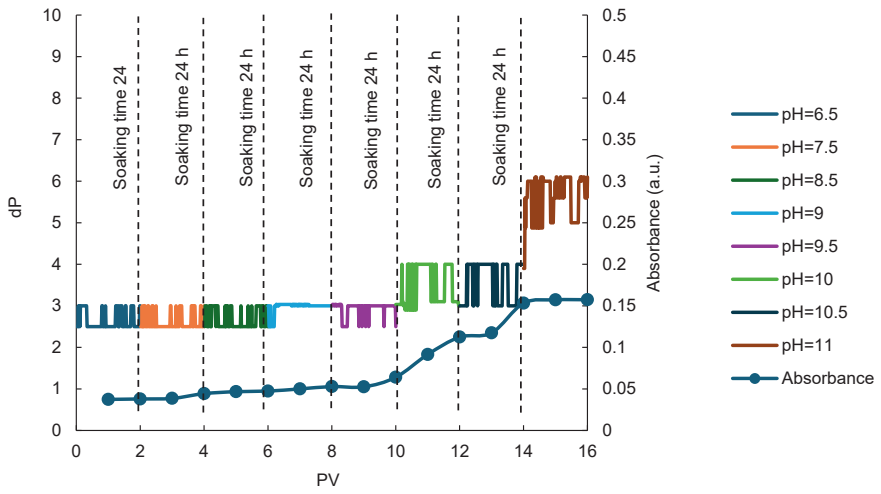


Fig. 6. Pressure drop and light absorbance changes at different pH levels at 0.25 M NaCl salinity.

Table 8
Experimental validation of critical pH predicted by DLVO theory.

Brine salinity	Modeled critical pH	Measured critical pH
0.2 M NaCl	8	9
0.25 M NaCl	10	10

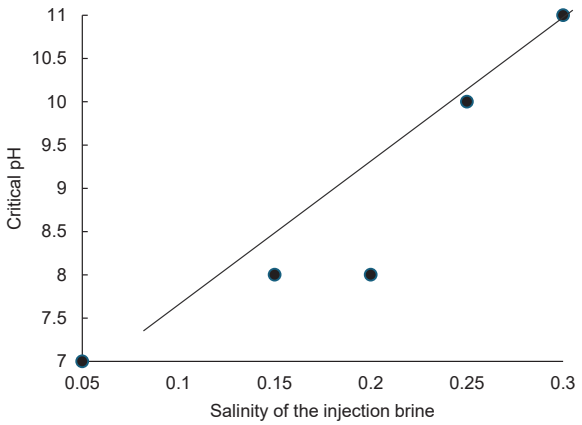


Fig. 7. Dependency of critical pH on the salinity of injected brine.

concentrations can mitigate the effects of pH changes, as ions from the brine help counteract increased hydroxide ions and stabilize the surface charge. As a result, fine particles in the reservoir rock remain stable.

4.2. Modeling of fines migration at the high injection rate

4.2.1. Prediction of critical flow rate by improved DLVO modeling

As the flow rate increases, the significance of hydrodynamic forces becomes more pronounced. As shown in Fig. 8, at a specific point, approximately 0.00001 m of fine particle radius, hydrodynamic forces exceed electrostatic and gravity forces. At this point, fines begin to migrate. The critical velocity is 0.0002 m/s. Additionally, the critical velocity decreases as the particle radius increases. This suggests that the effect of hydrodynamic forces on fine migration is influenced by particle size. For example, for a core sample and 0.25 M NaCl brine at

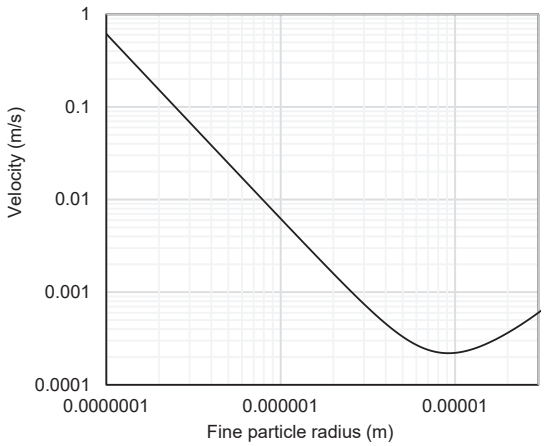


Fig. 8. Critical velocities for 0.25 M NaCl brine with pH of 8 dependent on fine particle radius.

pH 8 with a particle radius of 400 nm, the critical velocity was found to be 0.038 m/s, significantly higher than 0.0002 m/s. This indicates that the brine can flow through the rock more easily when pores are not obstructed by fine particles. However, as it is shown in Fig. 8, the detected correlation between critical velocity and particle size showed non-linear patterns. The mobilization of particles larger than 0.00001 m required advanced flow rates, because various forces interacted with hydrodynamic drag alongside particle-surface adhesion and pore geometry.

4.2.2. Confirmation of the model by the experiment

The coreflood test was conducted on the upper Berea sandstone core sample to assess the effect of hydrodynamic forces and determine the critical velocity for the given brine. During the test, three PVs of 0.25 M NaCl brine with pH 8 were injected at a rate of 0.2 cc/min. Simultaneously, pressure drop (dP) was monitored through the core for each injected PV, as shown in Fig. 8. Since the system's salinity decreased to 0.25 M, a 24-h soaking period was provided to allow sufficient contact between fine particles, the rock surface, and the injection brine. This soaking time also ensured stability in the interaction forces.

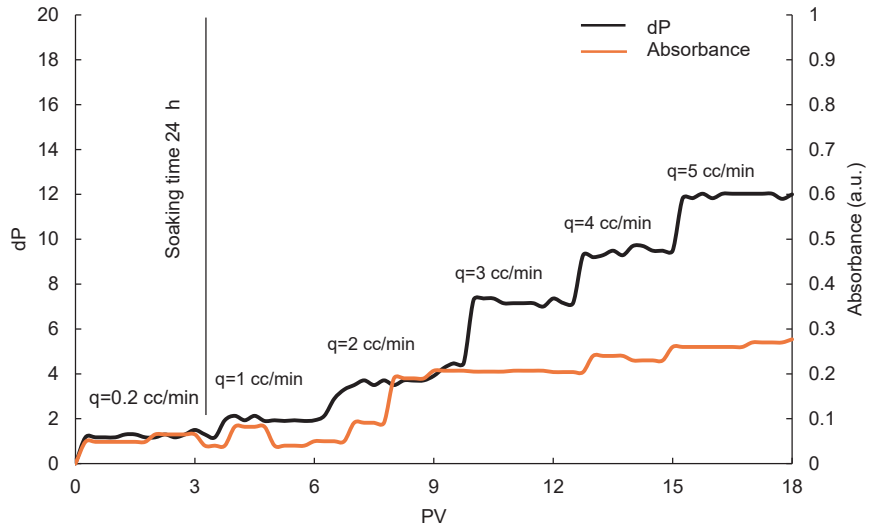


Fig. 9. Pressure drop and light absorbance change at pH = 8 for salinity 0.25 M NaCl.

Table 9
Critical flow at pH 8, 0.25 M NaCl.

Salinity (M)	pH	Modeled critical velocity (m/sec)	Measured critical flow rate (m/sec)
0.25	8	2.2×10^{-4}	1.9×10^{-4}

After this soaking period, the same brine was injected at an increased flow rate of 1 cc/min to examine the potential for fines migration caused by hydrodynamic forces. However, no fines detachment was observed at flow rates of 0.2 and 1 cc/min. When the flow rate was increased to 2 cc/min, a change in pressure drop was observed. Overall, the test showed a gradual change in flow rate and pressure drop, with 2 cc/min identified as the critical flow rate at which hydrodynamic forces were sufficient to initiate fines migration in the porous media system.

Absorbance measurements were taken for each PV to support the coreflood test results and confirm the presence of fines. At low flow rates (0.2 and 1 cc/min), the average absorbance of the effluent was low, nearly identical to that of the injection fluid. A change in absorbance was observed at the critical flow rate, with the absorbance values for each PV presented in Fig. 9.

4.2.3. Critical pH at a high rate

Although the critical flow rate is influenced by hydrodynamic forces, it is important to note that critical velocity is also affected by electrostatic interactions and gravity forces. Velocity is influenced by both attraction and repulsion forces, as well as the expansion of EDL. Consequently, it can be suggested that as pH increases or salinity decreases in the brine, the critical velocity may decrease. These electrostatic forces play a role in determining the critical pH at a given flow rate.

For the chosen pH value of 8 for 0.25 M NaCl brine, the critical flow rate was determined for both high and low rates. At low flow rates, the effect of attraction forces is more significant compared to repulsion forces. However, as the flow rate increases, the pH of 8 becomes critical for initiating fines migration. This is because hydrodynamic forces begin to dominate over both attraction and repulsion forces. As shown in Table 9, the velocity at which fines are released for the given pH was observed experimentally and by modeling, with results closely matching each other. Despite the dominance of hydrodynamic forces at higher flow rates, both interaction forces must be considered to estimate the velocity at which brine with a given pH is injected.

Another factor to consider when estimating parameters affecting fines release during brine injection at a specific flow rate is gravity force. Gravity force is influenced by the radius of the fine particles, as larger particles require more force to move. When considering brine injection parameters, the effect of gravity forces on fine particle initiation becomes more pronounced as flow rate or pH increases, while electrostatic attraction forces become less significant.

Error estimation in DLVO modeling for predicting the critical flow rate at which fines initially migrate involves examining uncertainties in input parameters such as zeta potential, particle size, and ionic strength, all of which affect DLVO interaction energies. The critical flow rate predicted at pH 8 and 0.25 M NaCl was evaluated against a calculated error of 13%. Variations in measured zeta potential under alkaline conditions and the sensitivity of double-layer repulsion energy to ionic strength contribute to this error. While a 13% error suggests moderate confidence in the model's ability to predict the critical flow rate, precise experimental measurements and a thorough understanding of surface charge forces in saline environments will be essential for improving accuracy.

The critical pH values for injected brines into sandstone cores confirm the high salinity conditions requiring higher alkalinity to stabilize particles and prevent the movement of small particles. The data coincide with DLVO-based predictions from Muneer et al. (2020), which defined salt concentrations as detachment thresholds for particles.

5. Conclusion

These studies aimed to predict critical pH and critical flow rate values using DLVO modeling. The DLVO model was applied to assess the interaction forces between sandstone rock surfaces and

fine particles within a given colloidal system. To validate the model, both modeling and experimental work were conducted at room temperature, considering a single-phase fluid flow.

The model successfully predicted the critical pH of the system, with experimental tests confirming its accuracy. Two types of brine salinity were used in the prediction, and for 0.2 M NaCl, fines migration begins at a pH of 8, whereas for 0.25 M NaCl, the critical pH rises to 10.

The next step involved integrating the DLVO model of electrostatic forces with hydrodynamic forces to predict the critical flow rate. The model accurately identified the flow rate threshold for fines migration initiation, with an error margin of 13%. It successfully captured the dynamics of fines detachment, demonstrating its robustness under varying fluid flow conditions. These findings underscore the validity of the DLVO theory as a reliable foundation for predicting reservoir operations and mitigating formation damage due to fines migration. The model was further validated by coreflood experiments conducted at various flow rates under single-phase flow conditions. Overall, the model provides a valuable tool for predicting fine particle release and movement during water injection into sandstone reservoirs with small clay particles on their surfaces.

While DLVO modeling proved successful in terms of predictive accuracy and alignment with experimental results, the approach still faces limitations, which have not been fully addressed in this study. Moving beyond these limitations is crucial to advancing the field, and future research will be key to overcoming these challenges. Several points should be discussed in the plan. (1) There is a need to control the temperature during the work since both zeta potential and pH is highly dependent on temperature. It may help measure parameters and forces between rocks and fines more accurately. In this work, the measured temperature was room temperature; however, to understand formation conditions, there might be a possibility to consider a reservoir temperature. (2) To predict critical pH, there were used only NaCl brine, which is a monovalent brine. Since DLVO modeling also depends on parameters such as ionic strength, there is a need to check its applicability by considering divalent brines as well as monovalent types of brine. (3) Most of the enhanced oil recovery methods are based on combining several methods into one. Therefore, there is a suggestion to integrate alkaline flooding with other methods such as Nanotechnology and check the critical parameters in these conditions. It can be effective since nanoparticles may positively affect the staying of fines on rock.

From the integration of the DLVO model's capability of predicting with the reservoir simulators, engineers and researchers can gain substantial information about the fluid–particle interactions in the system. With the integration of DLVO modeling with reservoir simulators, DLVO has additional uses besides oil recovery. This approach is crucial for modeling and controlling water movement in subsurface Sandstone aquifer systems. Sandstone formations are major aquifers, and quantitative estimates of water flow and transportation in these reservoirs are vital for successful water supply management.

CRediT authorship contribution statement

Elmira Dalabayeva: Writing – original draft, Validation, Methodology, Investigation, Data curation. **Peyman Pourafshary:** Writing – review & editing, Validation, Supervision, Formal analysis, Conceptualization. **Rizwan Muneer:** Writing – review & editing, Validation, Investigation.

Declaration of competing interest

The authors declare that they have no known competing financial interests or personal relationships that could have appeared to influence the work reported in this paper. All research was conducted independently and impartially at Nazarbayev University, with no external influence affecting the outcomes or interpretations presented in this manuscript.

References

Agi, A., Junin, R., Jaafar, M.Z., Majid, Z.A., Amin, N.A.S., Sidek, M.A., Yakasai, F., Zaini, M.A.A., Faizal, A.N.M., Gbadamosi, A., Sirajo, L., 2023. Dynamic stabilization of formation fines to enhance oil recovery of a medium permeability sandstone core at reservoir conditions. J. Mol. Liq. 371, 121107. https://doi.org/10.1016/j.molliq.2022.121107.

Ali, M., Al-Yaseri, A., Awan, F.U.R., Arif, M., Keshavarz, A., Iglauer, S., 2022. Effect of water-soluble organic acids on wettability of sandstone formations using streaming zeta potential and NMR techniques: implications for CO2 geo-sequestration. Fuel (Guildf.) 329, 125449. https://doi.org/10.1016/j.fuel.2022.125449.

Al-Sarihi, A., Zeinijahromi, A., Genolet, L., Behr, A., Kowollik, P., Bedrikovetsky, P., 2018, October. Fines migration as an EOR method during low salinity waterflooding. In: SPE Asia Pacific Oil and Gas Conference and Exhibition. https://doi.org/10.2118/192070-MS.

Barnaji, M.J., Pourafshary, P., Rasaie, M.R., 2016. Visual investigation of clay minerals' effects on oil recovery enhancement by low salinity water flooding. Fuel (Guildf.) 184, 826–835. https://doi.org/10.1016/j.fuel.2016.07.076.

Barouch, E., Matijević, E., Wright, T.H., 1987. Effects of Born repulsion on particle detachment. Chem. Eng. Commun. 55 (1–6), 29–40. https://doi.org/10.1080/00986448708911918.

Bradford, S.A., Torkzaban, S., Shapiro, A., 2013. A theoretical analysis of colloid attachment and straining in chemically heterogeneous porous media. Langmuir 29 (23), 6944–6952. https://doi.org/10.1021/la4011357.

Chavan, M., Dandekar, A., Patil, S., Khataniar, S., 2019. Low-salinity-based enhanced oil recovery literature review and associated screening criteria. Pet. Sci. 16 (6), 1344–1360. https://doi.org/10.1007/s12182-019-0325-7, 1344–1360.

Chequer, L., Nguyen, C., Loi, G., Zeinijahromi, A., Bedrikovetsky, P., 2021. Fines migration in aquifers: production history treatment and well behaviour prediction. J. Hydrol. 602, 126660. https://doi.org/10.1016/j.jhydrol.2021.126660.

Chrysikopoulos, C.V., Syngouna, V.I., 2014. Effect of gravity on colloid transport through water-saturated columns packed with glass beads: modeling and experiments. Environ. Sci. Technol. 48 (12), 6805–6813. https://pubs.acs.org/doi/abs/10.1021/es501295n.

Elimelech, M., 1995. Particle deposition and aggregation: measurement, modelling and simulation. http://ci.nii.ac.jp/ncid/BA70445796.

Gong, H., Li, Y., Dong, M., Ma, S., Liu, W., 2016. Effect of wettability alteration on enhanced heavy oil recovery by alkaline flooding. Colloids Surf., A 488, 28–35. https://doi.org/10.1016/j.colsurfa.2015.09.042.

Gregory, J., 1981. Approximate expressions for retarded van der Waals interaction. J. Colloid Interface Sci. 83 (1), 138–145. https://doi.org/10.1016/0021-9797(81)90018-7.

Israelachvili, J.N., 2011. Van der Waals forces between particles and surfaces. Elsevier eBooks, pp. 253–289. https://doi.org/10.1016/b978-0-12-375182-9.10013-2.

Johnson, W.P., Pazmino, E., Ma, H., 2009. Direct observations of colloid retention in granular media in the presence of energy barriers. Water Res. 44 (4), 1158–1169. https://doi.org/10.1016/j.watres.2009.12.014.

Karazincir, O., Williams, W., Rijken, P., 2017, October. Prediction of fines migration through core testing. In: SPE Annual Technical Conference and Exhibition. https://doi.org/10.2118/187157-MS.

Khilar, K.C., Fogler, H.S., 1984. The existence of a critical salt concentration for particle release. J. Colloid Interface Sci. 101 (1), 214–224. https://doi.org/10.1016/0021-9797(84)90021-3.

Kia, S.F., Fogler, H.S., Reed, M.G., 1987. Effect of pH on colloidally induced fines migration. J. Colloid Interface Sci. 118 (1), 158–168. https://doi.org/10.1016/0021-9797(87)90444-9.

Loeb, A.L., Overbeek, J.T.G., Wiersema, P.H., King, C.V., 1961. The electrical double layer around a spherical colloid particle. J. Electrochem. Soc. 108 (12), 269C. https://doi.org/10.1149/1.2427992.

Ma, Q., Li, H., Li, Y., 2020. The study to improve oil recovery through the clay state change during low salinity water flooding in sandstones. ACS Omega 5 (46), 29816–29829. https://pubs.acs.org/doi/10.1021/acsomega.0c03849.

Mansour, M., Moustafa, E.A., Eleraki, M., Noah, A., 2020. A novel approach of fines migration control using nanoparticle through zeta potential measurements. Pet. Coal 62 (3). https://www.researchgate.net/publication/343227182.

Mehdizad, A., Sedaee, B., Pourafshary, P., 2022. Visual investigation of the effect of clay-induced fluid flow diversion on oil recovery, as a low-salinity water flooding mechanism. J. Pet. Sci. Eng. 209, 109959. https://doi.org/10.1016/j.petrol.2021.109959.

Muneer, R., Hashmet, M.R., Pourafshary, P., 2020. Fine migration control in sandstones: surface force analysis and Application of DLVO Theory. ACS Omega 5 (49), 31624–31639. https://doi.org/10.1021/acsomega.0c03943.

Muneer, R., Hashmet, M.R., Pourafshary, P., 2022. DLVO modeling predicts critical salt concentration to initiate fine migration pre- and post-nanofluid treatment in sandstones. SPE J. (Soc. Pet. Eng. (U. S.), 1996) 27 (4), 1915–1929. https://doi.org/10.2118/209588-pa.

Muneer, R., Pourafshary, P., Hashmet, M.R., 2023. An integrated modeling approach to predict critical flow rate for fines migration initiation in sandstone reservoirs and water-bearing formations. J. Mol. Liq. 376, 121462. https://doi.org/10.1016/j.molliq.2023.121462.

Muneer, R., Pourafshary, P., Hashmet, M.R., 2024, February. Fines migration control in sandstone reservoirs: DLVO modeling for critical salt concentration and critical flow rate prediction. In: SPE Int. Conf. & Exhibition on Formation Damage Control. https://doi.org/10.2118/217870-MS.

Musharova, D., Mohamed, I.M., Nasr-El-Din, H.A., 2012. Detrimental Effect of Temperature on Fines Migration in Sandstone Formations. SPE Int. Symp. & Exhibition on Formation Damage Control. https://doi.org/10.2118/150953-MS.

Ohshima, H., Takeda, S.I., 2024. A new method for calculating the Hamaker constant based on the Hansen solubility parameters for nonpolar liquids. Colloids Interfaces 8 (2), 14. https://doi.org/10.3390/colloids8020014.

O'Neill, M.E., 1968. A sphere in contact with a plane wall in a slow linear shear flow. Chem. Eng. Sci. 23 (11), 1293–1298. https://doi.org/10.1016/0009-2509(68)89039-6.

Rosenbrand, E., Kjøller, C., Riis, J.F., Kets, F., Fabricius, I.L., 2015. Different effects of temperature and salinity on permeability reduction by fines migration in Berea sandstone. Geothermics 53, 225–235. https://doi.org/10.1016/j.geothermics.2014.06.004.

Russell, T., Chequer, L., Borazjani, S., You, Z., Zeinijahromi, A., Bedrikovetsky, P., 2018. Formation damage by fines migration. In: Formation Damage during Improved Oil Recovery. Elsevier, pp. 69–175. https://doi.org/10.1016/b978-0-12-813782-6.00003-8.

Saffman, P.G., 1965. The lift on a small sphere in a slow shear flow. J. Fluid Mech. 22 (2), 385–400. https://doi.org/10.1017/S0022112065000824.

Schumacher, G.A., van de Ven, T.G., 1987. Brownian motion of charged colloidal particles surrounded by electric double layers. Faraday Discuss. Chem. Soc. 83, 75–85. https://pubs.rsc.org/en/content/articlelanding/1987/dc/dc9878300075.

Sourani, S., Riazi, M., Kazemzadeh, Y., Fallah, H., 2014. A new approach for evaluating migration of nanoparticles in porous media. J. Dispersion Sci. Technol. https://doi.org/10.1080/01932691.2014.921859.

Trefalt, G., Borkovec, M., 2014. Overview of DLVO Theory. Laboratory of Colloid and Surface Chemistry, vol. 304. University of Geneva, Switzerland. https://docplayer.net/20731880-Overview-of-dlvo-theory.html.

Vaidya, R.N., Fogler, H.S., 1992. Fines migration and formation damage: influence of pH and ion exchange. SPE Prod. Eng. 7 (4), 325–330. https://doi.org/10.2118/19413-pa.

Wang, Y., Yu, M., Bo, Z., Bedrikovetsky, P., Le-Hussain, F., 2021. Effect of temperature on mineral reactions and fines migration during low-salinity water injection into Berea sandstone. J. Pet. Sci. Eng. 202, 108482. https://doi.org/10.1016/j.petrol.2021.108482.

Yan, Z., Huang, X., Yang, C., 2015. Deposition of colloidal particles in a microchannel at elevated temperatures. Microfluid. Nanofluidics 18, 403–414. https://doi.org/10.1007/s10404-014-1448-1.

Yang, Y., Yuan, W., Hou, J., You, Z., 2022. Review on physical and chemical factors affecting fines migration in porous media. Water Res. 214, 118172. https://doi.org/10.1016/j.watres.2022.118172.

You, Z., Badalyan, A., Yang, Y., Bedrikovetsky, P., Hand, M., 2019. Fines migration in geothermal reservoirs: laboratory and mathematical modeling. Geothermics 77, 344–367. https://doi.org/10.1016/j.geothermics.2018.10.006.